

$(p, p\alpha)$ cluster-knockout reaction on ${}^9\text{Be}$ at 200 MeV

A. Nadasen

*University of Michigan, Dearborn, Michigan 48128*P. G. Roos, N. S. Chant, C. C. Chang, G. Ciangaru,* H. F. Breuer, and J. Wesick[†]*University of Maryland, College Park, Maryland 20742*

E. Norbeck

University of Iowa, Iowa City, Iowa 52242

(Received 7 April 1989)

The $(p, p\alpha)$ cluster-knockout reaction on ${}^9\text{Be}$ has been investigated experimentally at a bombarding energy of 200 MeV. Coincident data were obtained at five quasifree angle pairs for proton angles ranging from 40° to 80° . The data were analyzed in terms of the distorted-wave impulse approximation. The calculated energy-sharing distributions reproduce the data reasonably well, indicating that the quasifree-knockout mechanism dominates the reaction. The factorization approximation employed in the calculation is found to be valid. The absolute spectroscopic factors derived from the data are in excellent agreement with lower-energy results, and compare well with shell-model predictions.

I. INTRODUCTION

The $(p, p\alpha)$ quasifree-knockout reaction has been used for several decades to investigate α clustering in nuclei. Nuclei studied range from ${}^6\text{Li}$ to ${}^{232}\text{Th}$.¹⁻³ The experiments have effectively used the flexibility of the three-body kinematics to obtain exact momentum matching. Thus the data were optimized for low momentum components of the cluster wave function, a region dominated by orbital angular momentum $L=0$ transfer. Extraction of absolute spectroscopic factors from the early studies was not possible because the data were generally analyzed using a plane-wave impulse approximation (PWIA),^{1,4} whereas distortion effects lead to large reductions in the cross sections, particularly at low energies.⁵ Introduction of the distorted-wave impulse approximation (DWIA) treatment of the reaction can, in principle, correct this deficiency and lead to the extraction of more meaningful parentage information for the α cluster.

However, there remain uncertainties and approximations associated with the DWIA analyses of the data. A concern at lower energies is the treatment of distortions. Figure 1 shows typical ratios of the peak distorted-wave cross section to plane-wave cross section as a function of bombarding energy for the $(p, p\alpha)$ reaction on several light elements. The proton angle is 60° . At low energies the ratio can be less than 10^{-3} . It is not clear how accurately the distorted-wave calculations include such huge effects. However, as the energy increases the distortion effects become less severe. By doubling the energy the distortion effects can be reduced by almost two orders of magnitude. Results at 100 MeV,^{2,3} which provide spectroscopic factors in good agreement with theoretical predictions, seem to indicate that the treatment of distortion effects are adequate. Thus studies of the $(p, p\alpha)$ reaction

at even higher energies are expected to provide quantitative information on cluster structure of nuclei with less uncertainties due to distortion effects.

The factorized form in which the DWIA calculations are carried out is also a concern. The $(p, p\alpha)$ triple-differential cross section is written as a product of the half-off energy-shell p - α cross section and the distorted momentum distribution of the α cluster. At 100 MeV (Refs. 2 and 6) and 150 MeV (Ref. 7) comparison of the angular distributions of the $(p, p\alpha)$ experimental data at zero recoil momentum with free p - α elastic scattering cross sections at the appropriate energies seem to support the validity of the factorization approximation. Tests at other energies would provide further evaluation of this procedure.

When a transition involves more than one value of L , unfolding the different contributions can be a problem. An interesting example is the ${}^9\text{Be}(p, p\alpha){}^5\text{He}$ (g.s.) reaction which proceeds from initial to final states having $J^\pi=3/2^-$. Thus orbital angular momenta of both $L=0$ and $L=2$ carried by the knocked-out α cluster are possible. Shell-model calculations⁸ predict equal contributions of these two components. However, the $L=0$ component peaks at the zero recoil momentum of the residual nucleus ($p_3=0$), while the $L=2$ term has minimum cross section at $p_3=0$ and peaks around $p_3=150$ MeV/ c . The $L=2$ contribution could not be unambiguously determined from the 100-MeV coplanar data² because the smearing due to distortion effects reduced the sensitivity to the higher momentum components. However, in non-coplanar measurements,⁹ where distortion effects were reduced, a value in close agreement with theory was obtained.

In view of the concerns outlined above, we decided to make measurements of the $(p, p\alpha)$ reaction on ${}^9\text{Be}$ at 200

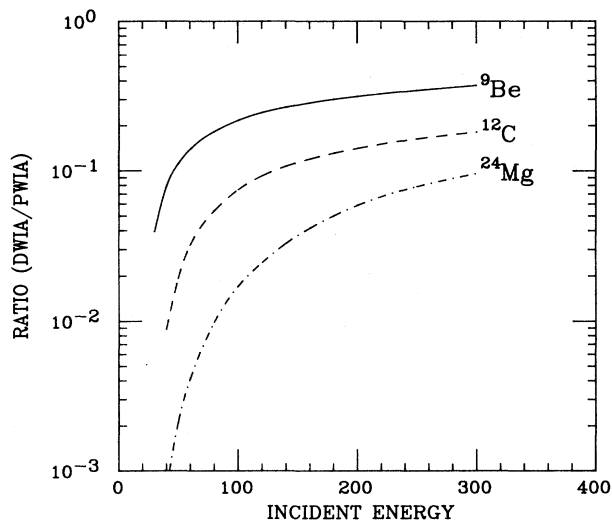


FIG. 1. Ratio of distorted-wave to plane-wave cross sections for the $(p, p\alpha)$ reaction on ${}^9\text{Be}$, ${}^{12}\text{C}$, ${}^{24}\text{Mg}$ at $p_3=0$ for a proton angle of 60° plotted as a function of bombarding energy.

MeV. An advantage of this higher energy is a further reduction in distortion effects, which should make it easier to unfold the $L=2$ component of the reaction. Also the factorization approximation could be evaluated at a higher energy where off-shell effects are expected to be less severe. In addition, these data will also be able to determine the energy dependence, if any, of the various components of the reaction mechanism.

Section II describes the experimental procedure. The results of the measurements are given in Sec. III. The DWIA analysis of the data is presented in Sec. IV. In Sec. V we provide a summary of our results and conclusions.

II. EXPERIMENT

Measurements were carried out utilizing a 200-MeV proton beam at the Indiana University Cyclotron Facility which was momentum analyzed ($\Delta E/E=0.05\%$) and focused on a 2.5-mg cm^{-2} self-supporting ${}^9\text{Be}$ target at the center of a 1.6-m diameter scattering chamber. The beam spot on target was approximately $3\text{ mm} \times 3\text{ mm}$ with a current between 7 and 40 nA, depending on the detector angles.

The proton and alpha telescopes were placed on remote-controlled arms on either side of the beam in a coplanar geometry. The proton telescope consisted of a 1-mm Si surface-barrier ΔE detector followed by a $7.6\text{-cm} \times 7.6\text{-cm} \times 12.7\text{-cm}$ thick NaI(Tl) stopping detector. A 4.7-cm thick lead slit with a 1.6-cm diameter aperture defined a solid angle of 5.95 msr. The alpha telescope consisted of a $200\text{-}\mu\text{m}$ Si ΔE and a 5-mm Si(Li) E detector followed by a 1-mm Si detector used to veto particles passing through the E counter. This telescope had an identical lead slit for cleanup and a solid angle defining slit made of 1.6-cm-thick brass with a 0.95-cm diameter hole, subtending 1.83 msr. This system permitted mea-

surement of protons from 15 to 200 MeV and alphas from 20 to 150 MeV.

The outputs of all detectors were amplified and fed to 8192 channel CAMAC analog-to-digital converters. Coincidences between the two telescopes were detected using a time-to-digital converter (TDC) with an overall time resolution of about 2 ns, easily separating beam bursts. The TDC range of 200 ns permitted the accumulation of both real and random coincidences simultaneously.

Pulsar signals generated at a rate proportional to the beam current were fed to all preamplifiers and used to correct the data for gain shifts in the NaI and loss of events due the dead time of the system.

All detectors were calibrated over their dynamic ranges using radioactive sources and proton scattering from ${}^2\text{H}$ and ${}^{12}\text{C}$. The accuracy of angular positioning of the scattering chamber arms was determined by measuring coincidences from $p+d$ elastic scattering. One- and two-dimensional arrays of the data were created for on-line monitoring of dead time, pileup, detector gains, random rates, particle identification (PID), and statistics of true knockout data. All data were written event by event to magnetic tapes for later off-line analyses. Data-monitoring scalars were also written on the event tapes.

III. EXPERIMENTAL RESULTS

Measurements were made at five angle pairs. The proton angles for these measurements were 40° , 50° , 60° , 70° , and 80° . In each case the alpha angle was chosen to permit zero recoil momentum of the residual ${}^5\text{He}$, thus defining a so-called "quasifree" angle pair. The ΔE vs E spectra showed clean separation of particle species for both telescopes. Windows for protons and alpha particles were selected and random coincident events were subtracted with the aid of windows on the TDC spectrum. Energy addition of the ΔE and E signals was carried out by software.

For each angle pair, a two-dimensional coincidence spectrum of proton energies versus alpha energies was created. A calculated kinematic locus displayed on this two-dimensional array was used to determine the true quasifree-knockout events. These were then projected onto the proton energy axis, resulting in an energy-sharing distribution. The energy-sharing distributions obtained for the five angle pairs are shown in Figs. 2–6. Since a single setup was used for the entire experiment, the relative uncertainties are dominated by statistical errors. Uncertainties from other sources are estimated to be $\sim 5\%$. The errors indicated in Figs. 2–6 are statistical. Absolute errors in the data from all sources are estimated to be less than 10%.

The data are characterized by a broad peak centered around the zero-recoil-momentum point of the residual nucleus, which is indicated by an arrow in each energy-sharing distribution. This is evidence of the dominance of the $L=0$ component of the reaction in this region. The cross sections in the higher-momentum regions are largely due to the $L=2$ component.

It is observed that the quasifree peak moves to lower

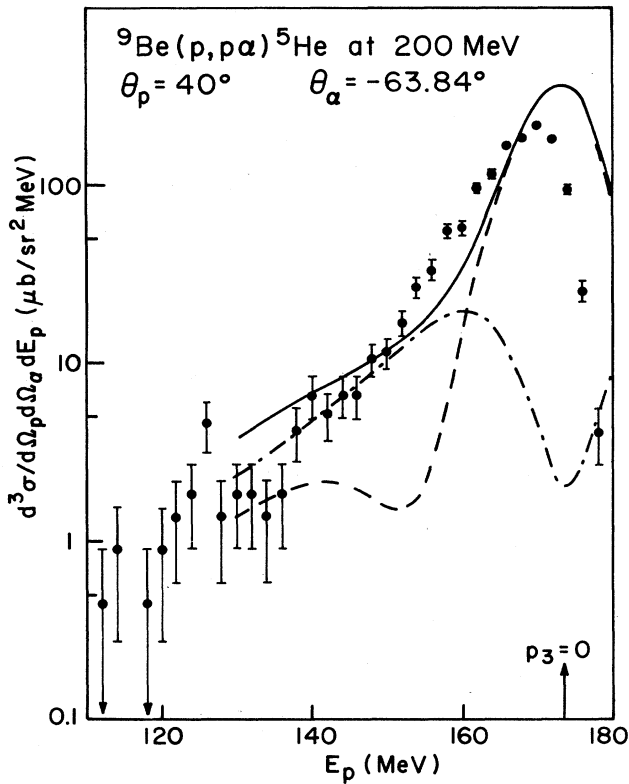


FIG. 2. Energy-sharing distribution for the ${}^9\text{Be}(p, p\alpha){}^5\text{He}$ reaction at angle pair $\theta_p/\theta_\alpha=40^\circ/-63.84^\circ$. The curves represent DWIA calculations for $L=0$ (dashed), $L=2$ (dot-dashed), and their incoherent sum (solid), normalized to the data.

proton energies as the proton angle increases. As expected, this shift follows the free p - α elastic scattering kinematics. This displacement of the quasifree peak downward in energy helps to separate the true quasifree-knockout events from other competing processes. For example, as the proton angle is increased the development of a secondary peak around $E_p=155$ MeV is noticed. This appears to be due to sequential α emission, arising from inelastic excitations of the ${}^9\text{Be}$ nucleus to about 40 MeV followed by α decay. This rather surprising behavior has also been noted in other studies of ${}^9\text{Be}(p, p\alpha)$. The cross section for this peak, estimated from the larger proton-angle data, is about $20\pm 5 \mu\text{b}/\text{sr}^2$ with a very weak angle dependence.

At our most forward proton angle of 40° , the peak of the distribution appears to be about 3 MeV below the $p_3=0$ point. It appears to be due to an instrumental effect leading to loss of events for $E_p > 170$ MeV. Thus, we believe we may be missing part of the quasifree peak for this angle pair—probably due to threshold effects in the alpha telescope.

IV. ANALYSIS

The data were analyzed in terms distorted-wave impulse approximation (DWIA) calculations carried out using the computer code THREEDIE.¹⁰ In the factorized

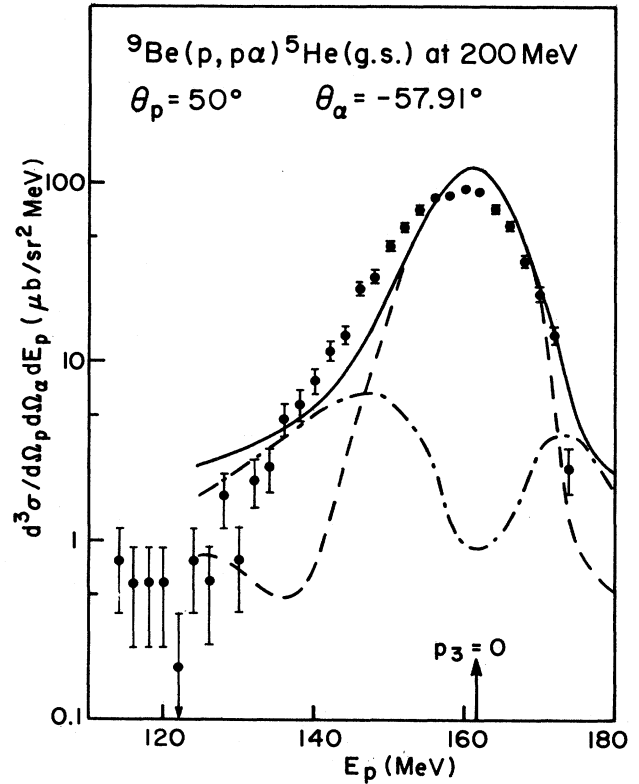


FIG. 3. Energy-sharing distribution for the ${}^9\text{Be}(p, p\alpha){}^5\text{He}$ reaction at angle pair $\theta_p/\theta_\alpha=50^\circ/-57.91^\circ$. The curves represent DWIA calculations for $L=0$ (dashed), $L=2$ (dot-dashed), and their incoherent sum (solid), normalized to the data.

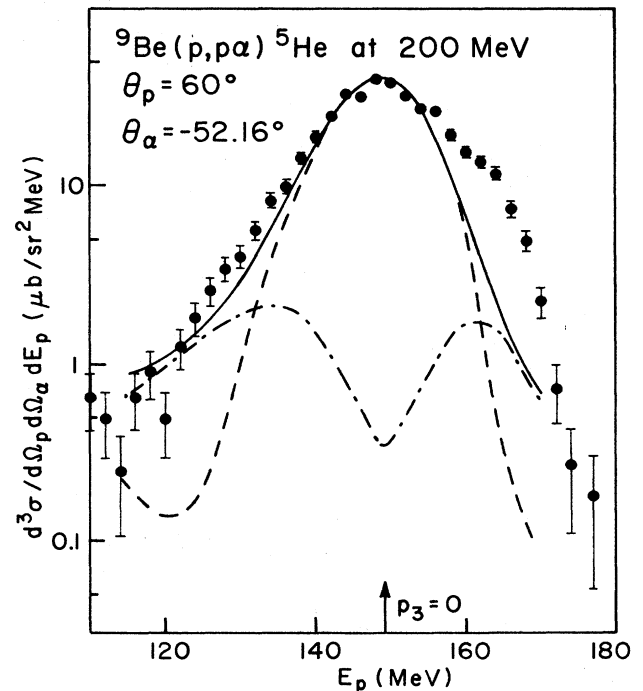


FIG. 4. Energy-sharing distribution for the ${}^9\text{Be}(p, p\alpha){}^5\text{He}$ reaction at angle pair $\theta_p/\theta_\alpha=60^\circ/-52.16^\circ$. The curves represent DWIA calculations for $L=0$ (dashed), $L=2$ (dot-dashed), and their incoherent sum (solid), normalized to the data.

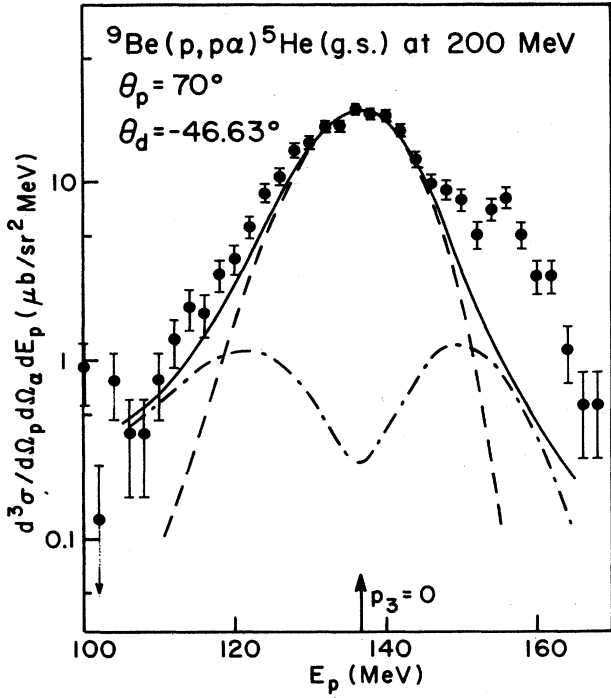


FIG. 5. Energy-sharing distribution for the ${}^9\text{Be}(p, p\alpha){}^5\text{He}$ reaction at angle pair $\theta_p/\theta_\alpha = 70^\circ/-46.63^\circ$. The curves represent DWIA calculations for $L=0$ (dashed), $L=2$ (dot-dashed), and their incoherent sum (solid), normalized to the data.

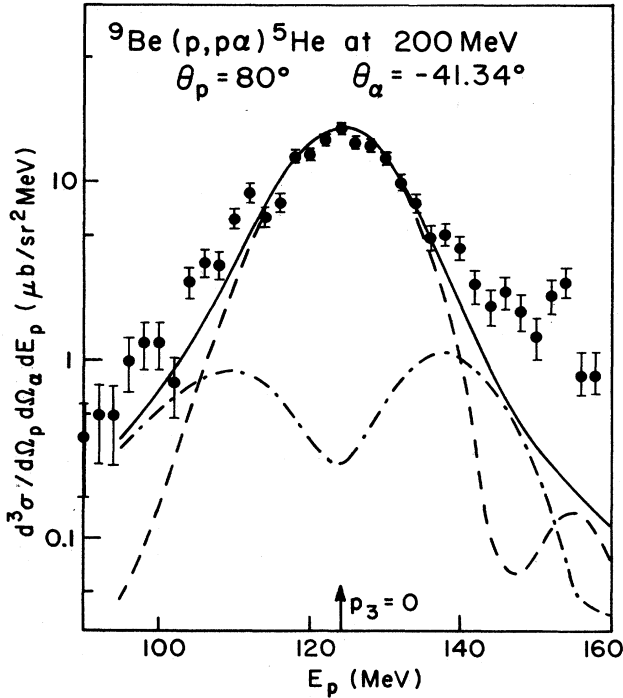


FIG. 6. Energy-sharing distribution for the ${}^9\text{Be}(p, p\alpha){}^5\text{He}$ reaction at angle pair $\theta_p/\theta_\alpha = 80^\circ/-41.34^\circ$. The curves represent DWIA calculations for $L=0$ (dashed), $L=2$ (dot-dashed), and their incoherent sum (solid), normalized to the data.

form of the DWIA the triple-differential cross section can be written as

$$\frac{d^3\sigma}{d\Omega_p d\Omega_\alpha dE_p} = F_k S_\alpha \left[\sum_\lambda |T_{BA}^{\alpha L \lambda}|^2 \right] \frac{d\sigma}{d\Omega_{p-\alpha}}, \quad (1)$$

where F_k is a kinematic factor and S_α is an α spectroscopic factor. The quantity $d\sigma/d\Omega_{p-\alpha}$ represents the two-body interaction between the projectile and the ejected α cluster. This is properly a half-off energy-shell interaction because the α cluster is bound in the target nucleus. However, since the α - ${}^5\text{He}$ binding energy is small compared to the incident proton energy, it was approximated by the free two-body cross section at the final relative energy of the p - α system. This procedure has been found to be satisfactory² at 100 MeV. The quantity $T_{BA}^{\alpha L \lambda}$ is written as

$$T_{BA}^{\alpha L \lambda} = (2L+1)^{-1/2} \times \int \chi_p^{(-)*}(\mathbf{r}) \chi_\alpha^{(-)*}(\mathbf{r}) \chi_p^{(+)}(\mathbf{r}) \Upsilon \phi_{L\lambda}^\alpha(\mathbf{r}) d\mathbf{r}, \quad (2)$$

where $\Upsilon = B/A$, the ratio of the residual to target nucleus mass numbers. the χ 's are distorted waves for the incoming and outgoing particles and $\phi_{L\lambda}^\alpha$ is the "bound-state wave function" of the α cluster resulting from projecting the ${}^9\text{Be}$ wave function onto a product of α and ${}^5\text{He}$ wave functions.

The optical-model potential parameters used in the calculations are listed in Table I. Previous investigations^{2,3,9} have indicated that the shape of the calculated energy-sharing distributions is essentially the same for different distorting potentials and that the predicted magnitude changes by at most 25%. Thus it may be appropriate to assume that uncertainties in the derived spectroscopic information due to improper choice of distorting potentials are at most 25%.

The α cluster bound-state wave function was approximated by solving the bound-state problem in a Woods-Saxon potential with geometrical parameters obtained from folding model calculations² and a well depth adjusted to reproduce the empirical separation energy of the α cluster from the ${}^5\text{He}$ core. The principal quantum number N for the bound-cluster wave function was chosen on the basis of conservation of harmonic-oscillator shell-model quanta. Thus $N=3$ and 2 for $L=0$ and 2 transitions, respectively.

It is important to verify that the factorization approximation implicit in Eq. (1) is indeed valid for the reaction. The triple-differential cross section on the left-hand side of Eq. (1) is angle dependent due to the quantities F_k and $d\sigma/d\Omega_{p-\alpha}$. Explicit DWIA calculations show that $|T_{BA}^{\alpha L \lambda}|^2$ varies by less than $\pm 10\%$ at the $p_3=0$ point over the angular range studied in this investigation. It is thus appropriate to modify Eq. (1) to the form

$$\frac{d^3\sigma}{d\Omega_p d\Omega_\alpha dE_p} / F_k = S_\alpha \left[\sum_\lambda |T_{BA}^{\alpha L \lambda}|^2 \right] \frac{d\sigma}{d\Omega_{p-\alpha}}. \quad (3)$$

For $p_3=0$, the quantity on the left-hand side of Eq. (3) is expected to be proportional to the free two-body p - α cross sections near 200 MeV, except for variations due to distortion effects. A comparison is made in Fig. 7. The

TABLE I. Optical potential parameters used in the DWIA calculations.

System	V	r_0	a_0	W	r_w	a_w	r_c	Reference
$p + {}^9\text{Be}$	13.86	1.11	0.713	10.78	1.0	0.855	1.12	11
$p + {}^5\text{He}$	16.96	1.11	0.713	10.78	1.0	0.855	1.12	11
$\alpha + {}^5\text{He}$	107.0	1.14	0.700	1.00	1.14	0.700	1.14	12
Bound state	89.0	1.35	0.73				1.35	2

solid lines represent measured free p - α cross sections at 156 (Ref. 13), 200 and 350 MeV (Ref. 14). The experimental $(p, p\alpha)$ triple-differential cross sections at $p_3=0$ divided by the kinematic factor, plotted as a function of the center-of-mass angle of the outgoing p - α system, are shown as points. All points have a single normalization, determined from the largest scattering angle. The agreement with free p - α scattering at 200 MeV, particularly for the larger angles, is very good. The somewhat low value of the 40° - 63.84° datum point may be due to a loss of lower-energy α particles due to the detector limitations discussed in Sec. III. Overall the results of this comparison are encouraging and seem to indicate that the factorization approximation works very well at 200 MeV.

Both $NL=3S$ and $2D$ calculations were carried out for each angle pair, and normalized to the data in order to determine an experimental spectroscopic factor. Since the $L=2$ component is small near the $p_3=0$ point, the $L=0$ calculations were first normalized at the $p_3=0$ point for all five angle pairs to obtain a single $L=0$ spectroscopic factor. The data for the three largest proton angles were given more weight in the determination of

this normalization, because these data seem to have less interference from other effects. The value extracted was 0.45, which is in excellent agreement with results at 100 (Refs. 2 and 9) and 150 MeV,⁷ but is $\sim 20\%$ lower than the theoretical prediction (0.56) of Kurath.⁸ Next the $L=2$ calculations were normalized, such that the sum of the two contributions best reproduced the shape of the energy-sharing distributions. The derived spectroscopic factor for the $2D$ term was 0.55, in excellent agreement with previous experimental results and with Kurath's calculations (0.55). The calculations normalized with these common extracted spectroscopic factors are shown in Figs. 2-6.

It is observed that the calculations reproduce the shape of the energy-sharing distributions reasonably well. Major discrepancies exist in the higher energy side of the three large proton-angle data. As already noted, this appears to be due to sequential processes.

V. SUMMARY AND CONCLUSION

We have made measurements of the $(p, p\alpha)$ reaction on ${}^9\text{Be}$ at a bombarding energy of 200 MeV. Energy-sharing distributions were obtained for five quasifree angle pairs ranging from $\theta_p=40^\circ$ to 80° . Each energy-sharing spectrum shows a prominent quasifree-knockout peak dominated by the $L=0$ component of the reaction. The $L=2$ component results in a broadening of the distribution. The angular distribution of the quasifree peak is in good agreement with free p - α cross sections at 200 MeV. This result provides confirmation that the factorization approximation used in the calculations is indeed valid.

The DWIA calculations reproduce the shapes of the energy-sharing distributions reasonably well, except for regions where sequential decays contribute to the cross section. The derived spectroscopic factors of 0.45 for $L=0$ and 0.55 for $L=2$ are in excellent agreement with results at lower energies. While the $L=2$ spectroscopic factor agrees with theoretical predictions, the $L=0$ spectroscopic factor is $\sim 20\%$ lower. Because of less severe distortions as a result of using a higher bombarding energy, a more reliable determination of the $L=2$ spectroscopic factor was possible. Our results seem to confirm that the DWIA provides a satisfactory description of the $(p, p\alpha)$ reaction at 200 MeV.

ACKNOWLEDGMENTS

We wish to thank the Indiana University Cyclotron Facility (IUCF) cyclotron staff for providing the high quality proton beams for this experiment. This work was supported in part by the National Science Foundation.

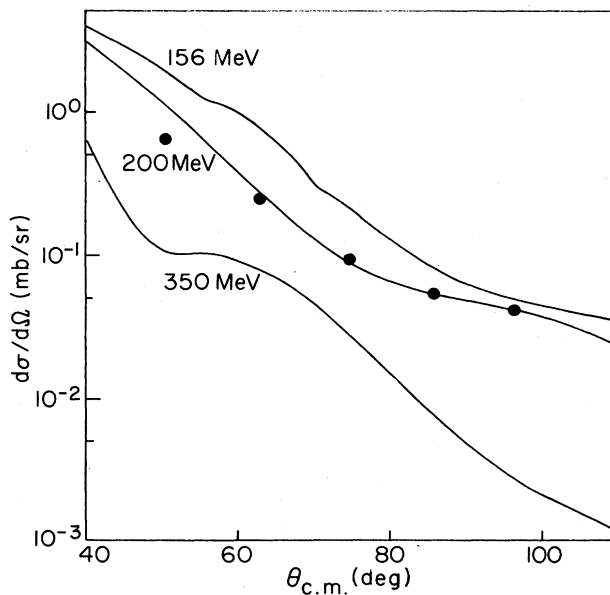


FIG. 7. Half-off-shell p - α cross sections extracted from the ${}^9\text{Be}(p, p\alpha){}^5\text{He}$ reaction at 200 MeV. The solid lines represent measured free p - α elastic scattering cross sections at 156, 200, and 350 MeV.

*Present address: Schlumberger Well Services—Engineering, Houston, TX 77210.

†Present address: Department of Radiology, University of Washington, Seattle, WA 98195.

¹D. Bachelier, M. Bernas, O. M. Bilaniuk, J. L. Boyard, J. C. Jourdain, and P. Radvanyi, *Phys. Rev. C* **7**, 165 (1973).

²P. G. Roos, N. S. Chant, A. A. Cowley, D. A. Goldberg, H. D. Holmgren, and R. Woody III, *Phys. Rev. C* **15**, 69 (1977).

³T. A. Carey, P. G. Roos, N. S. Chant, A. Nadasen, and H. L. Chen, *Phys. Rev. C* **29**, 1273 (1984).

⁴P. G. Roos, H. G. Pugh, M. Jain, H. D. Holmgren, M. Epstein, and C. A. Ludemann, *Phys. Rev.* **176**, 1246 (1968).

⁵J. S. Watson, H. G. Pugh, P. G. Roos, D. A. Goldberg, D. I. Bonbright, and R. A. J. Riddle, *Nucl. Phys.* **A172**, 513 (1971), and references therein.

⁶P. G. Roos, D. A. Goldberg, N. S. Chant, R. Woody III, and

W. Reichart, *Nucl. Phys.* **A257**, 317 (1976).

⁷C. W. Wang, P. G. Roos, N. S. Chant, G. Ciangaru, F. Khaizaie, D. J. Mack, A. Nadasen, S. J. Mills, and R. E. Warner, *Phys. Rev. C* **31**, 1662 (1985).

⁸D. Kurath, *Phys. Rev. C* **7**, 1390 (1973).

⁹A. Nadasen, N. S. Chant, P. G. Roos, T. A. Carey, R. Cowen, C. Samanta, and J. Wesick, *Phys. Rev. C* **22**, 1394 (1980).

¹⁰N. S. Chant and P. G. Roos, *Phys. Rev. C* **15**, 57 (1977).

¹¹G. L. Moake and P. T. Debevec, *Phys. Rev. C* **21**, 25 (1980).

¹²G. Igo, *Phys. Rev.* **117**, 1079 (1960).

¹³V. Comparat, R. Frascaria, N. Fujiwara, N. Marty, M. Morlet, P. G. Roos, and A. Willis, *Phys. Rev. C* **12**, 251 (1975).

¹⁴G. A. Moss, L. G. Greeniaus, J. M. Cameron, D. A. Hutcheon, R. L. Liljestrang, C. A. Miller, G. Roy, B. K. S. Koene, W. T. H. van Oers, A. W. Stetz, A. Willis, and N. Willis, *Phys. Rev. C* **21**, 1932 (1980).